

Nematic Torques in Scalar Active Matter: When Fluctuations Favor Polar Order and Persistence

Gianmarco Spera¹, Charlie Duclut^{1,2}, Marc Durand¹, and Julien Tailleur^{3,1}

¹*Université Paris Cité, Laboratoire Matière et Systèmes Complexes (MSC), UMR 7057 CNRS, F-75205 Paris, France*

²*Laboratoire Physique des Cellules et Cancer (PCC), CNRS UMR 168, Institut Curie, Université PSL, Sorbonne Université, 75005 Paris, France*

³*Department of Physics, Massachusetts Institute of Technology, Cambridge, Massachusetts 02139, USA*

 (Received 17 January 2023; revised 12 July 2023; accepted 8 January 2024; published 13 February 2024)

We study the impact of nematic alignment on scalar active matter in the disordered phase. We show that nematic torques control the emergent physics of particles interacting via pairwise forces and can either induce or prevent phase separation. The underlying mechanism is a fluctuation-induced renormalization of the mass of the polar field that generically arises from nematic torques. The correlations between the fluctuations of the polar and nematic fields indeed conspire to increase the particle persistence length, contrary to what phenomenological computations predict. This effect is generic and our theory also quantitatively accounts for how nematic torques enhance particle accumulation along confining boundaries and opposes demixing in mixtures of active and passive particles.

DOI: [10.1103/PhysRevLett.132.078301](https://doi.org/10.1103/PhysRevLett.132.078301)

Active matter describes systems comprising elementary units able to exert nonconservative forces on their environment [1–4]. Such systems are ubiquitous in nature [5–8] and can also be engineered in the lab [9–12], paving the way towards the engineering of soft active materials. A key requirement to do so is the ability to predict how microscopic characteristics of active systems impact their emerging behaviors. However, we still lack a statistical mechanics treatment generalizing what is classically done for equilibrium systems.

Following pioneering works [13,14], progress has been made over the past fifteen years to account for the large-scale properties of “simple” active systems, in which self-propulsion interplays with a single other ingredient, be it aligning torques [3,15,16], external potentials [17–22], pairwise forces [23–32], or mediated interactions [33–36]. However, realistic systems typically involve many of these aspects simultaneously and the resulting physics is both much richer and much harder to account for [37–41]. In particular, the interplay between pairwise forces and aligning torques has attracted a lot of interest recently [3,42–50].

Aligning interactions obviously play a crucial role in the ordered phases they induce, where they lead to a wealth of dynamical patterns that have been extensively studied [3]. Their impact in the disordered phase, on the contrary, remains largely unexplored. For concreteness, we work in $d = 2$ dimensions and consider N active particles of positions \mathbf{r}_i and orientations $\mathbf{u}_i = (\cos \theta_i, \sin \theta_i)$ evolving as

$$\dot{\mathbf{r}}_i = v_0 \mathbf{u}_i + \mu \sum_{\langle j,i \rangle} \mathbf{F}_{ji} + \sqrt{2D_t} \boldsymbol{\eta}_i, \quad (1a)$$

$$\dot{\theta}_i = \frac{\gamma}{n_i} \sum_{\langle j,i \rangle} \sin[p(\theta_j - \theta_i)] + \sqrt{2D_r} \zeta_i, \quad (1b)$$

where v_0 is the particle self-propulsion velocity, μ is the particle mobility, D_t is the translational diffusivity, $\boldsymbol{\eta}_i$ and ζ_i are centered unit-variance Gaussian white noises, and \mathbf{F}_{ji} is the force exerted by particle j onto particle i . Particles interact when their distance is smaller than r_0 and $n_i = \sum_{\langle j,i \rangle} 1$ is the number of particles interacting with particle i . One usually refers to the aligning interactions as polar when $p = 1$ and nematic when $p = 2$, consistent with the symmetry of the ordered phase they favor. Finally, γ is the alignment strength and D_r is the rotational diffusivity, which controls the microscopic persistence time $\tau = D_r^{-1}$.

The role of aligning interactions in the disordered phase can be analyzed from symmetry considerations. Particle conservation makes the density field a hydrodynamic mode, whose evolution is governed by a density current: $\partial_t \rho(\mathbf{r}, t) = -\nabla \cdot \mathbf{j}(\mathbf{r}, t)$. The latter includes an advective contribution $v_0 \mathbf{m}$ due to self-propulsion, where $\mathbf{m}(\mathbf{r}, t)$ is the orientation field of the particles. Since polar torques ($p = 1$) align the particle orientations, they control the particle persistence [45] and lead to an evolution for \mathbf{m} reminiscent of a Landau theory: $\partial_t \mathbf{m} = -(T - T_c) \mathbf{m} + [\dots]$, where $[\dots]$ refers to transport terms and higher-order contributions. The collective persistence time of the advective current due to self-propulsion thus scales as $\tau^c = (T - T_c)^{-1}$

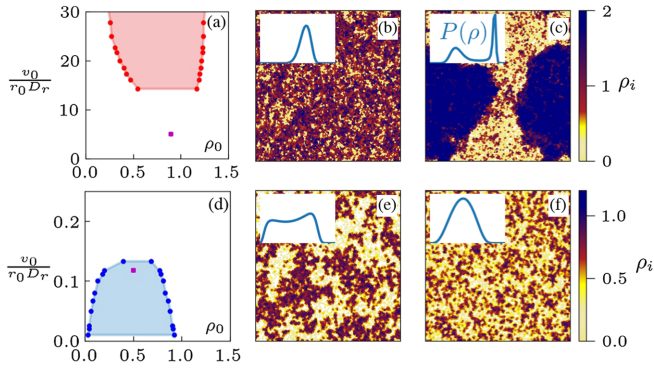


FIG. 1. Impact of nematic torques on the phase separation of active particles evolving under Eq. (1). Particles interact via either purely repulsive Weeks-Chandler-Andersen potential (top) or Lennard-Jones potential (bottom). (a),(d) Phase diagrams as the average density ρ_0 and the rotational diffusivity D_r are varied, in absence of nematic torques. Shaded regions correspond to phase-separated systems and are delimited by coexistence lines (symbols). (b),(e) Snapshots corresponding to the magenta squares in (a),(d). (c),(f) Snapshots obtained from (b),(e) upon the addition of nematic torques: $\gamma = 6.5D_r$ in (c) and $\gamma = 5.9D_r$ in (f). The color of particle i encodes $\rho_i = n_i/(\pi r_0^2)$. Global nematic order is observed for $\gamma \gtrsim 7D_r$. Insets in (b),(c),(e),(f) show histograms of the local density. Bimodality signals phase separation. Nematic torques induce MIPS in (c) starting from the homogeneous phase seen at $\gamma = 0$ in (b). They destroy in (f) the near-equilibrium phase separation shown in (e) that results from the attractive tail of the Lennard-Jones potential.

in the disordered (or “high-temperature”) phase: polar torques enhance persistence by decreasing the “mass” (that is to say, the large-scale limit of the inverse relaxation time of fluctuations) of the polar field. Immediately, this implies that aligning interactions can promote collective behaviors such as motility-induced phase separation (MIPS) [23–32,34] by lowering the critical “bare” persistence length v_0/D_r above which MIPS can be observed [45,50].

Nematic torques ($p = 2$) are ubiquitous among active particles since polar shapes generically lead to nematic alignment upon collisions. The symmetry argument presented above for the polar case does not predict anything interesting for the nematic case: to leading order, the Landau theory reads $\partial_t \mathbf{m} = -D_r \mathbf{m} + \kappa \mathbf{m} \cdot \mathbf{q} + [\dots]$, where \mathbf{q} is the nematic order parameter and κ is proportional to the amplitude of the nematic torques. In the high-temperature phase, $\mathbf{q} = 0$ and mean-field theory predicts that nematic torques do not impact the particle persistence [50], hence leaving their emerging behaviors unaltered. While the ordered phases induced by nematic torques have attracted a lot of attention [3,51–56], the impact of nematic alignment on disordered scalar active matter has thus been little studied.

In this Letter, we show that taking fluctuations into account leads to a much richer scenario than reported so far and that nematic torques can either induce or destroy phase separation in scalar systems, as illustrated in Fig. 1 (all our

simulations are detailed in [57]). Our central result is the discovery of the underlying mechanism: the aligning nematic torques reduce, through fluctuations, the mass of the polar field. In turn, this enhances polar order and particle persistence length, which plays an important role in controlling the emergent properties. We note that fluctuations lower the critical temperature in aligning spin systems [65] so that this effect is the opposite of what one would naively imagine. It is also the opposite of what a phenomenological computation starting from a Landau theory would predict. Instead, it relies on the precise correlations of the fluctuations affecting polar and nematic fields.

To proceed, we construct the coupled stochastic field theory describing the dynamics of the density, polar and nematic fields emerging from Eq. (1). Using a weak-noise expansion, we show that the correlated fluctuations of polar and nematic fields conspire to lower the mass of the polar field. To test this prediction, we consider the accumulation of self-propelled particles against confining boundaries in the absence of pairwise forces. Nematic torques then lead to an enhanced accumulation, which is quantitatively accounted for by the renormalization of the persistence length. Then, we consider repulsive forces between particles and develop a new theory for the spinodal decomposition of MIPS in the presence of aligning torques. We show that nematic alignment enhances the active contribution to a generalized bulk modulus, which becomes negative and induces MIPS for strong enough alignment. Finally, we show that our results hold for more general systems and that nematic torques enhance the persistence of active particles in mixtures of active and passive particles as well as in a nematic version of the Vicsek model. For mixtures, the enhancement of the particle persistence length is strong enough to suppress demixing.

Fluctuation-induced increase of the persistence length.— Starting from the microscopic dynamics, Eq. (1), stochastic calculus allows deriving the time evolution of the empirical measure $\hat{\psi}(\mathbf{r}, \theta) = \sum_i \delta(\mathbf{r} - \mathbf{r}_i) \delta(\theta - \theta_i)$, whose Fourier modes $\hat{f}_k \equiv \int d\theta \hat{\psi}(\mathbf{r}, \theta) e^{ik\theta}$ describe the fluctuating hydrodynamic fields of the model. The particle density field indeed corresponds to $\hat{\rho}(\mathbf{r}) = \hat{f}_0(\mathbf{r})$ while $\hat{f}_1(\mathbf{r}) = \hat{m}_x(\mathbf{r}) + i\hat{m}_y(\mathbf{r})$ encodes the orientation field $\hat{\mathbf{m}}(\mathbf{r}) = \sum_i \mathbf{u}(\theta_i) \delta(\mathbf{r} - \mathbf{r}_i)$. The local nematic order is quantified by $\hat{f}_2(\mathbf{r}) = 2\hat{q}_{xx}(\mathbf{r}) + i2\hat{q}_{xy}(\mathbf{r})$ [66]. For simplicity, we set $D_t = 0$ but our results hold for finite D_t . Assuming that $\hat{\psi}$ varies over scales larger than the interaction range r_0 , standard algebra leads to the following time evolution for \hat{f}_k [57]:

$$\begin{aligned} \partial_t \hat{f}_k + \frac{v_0}{2} (\nabla^* \hat{f}_{k+1} + \nabla \hat{f}_{k-1}) + \mu \nabla \cdot \hat{\mathbf{I}}_k \\ = -k^2 D_r \hat{f}_k + \frac{k\gamma}{2\hat{f}_0} (\hat{f}_2 \hat{f}_{k-2} - \hat{f}_{-2} \hat{f}_{k+2}) + \xi_k, \end{aligned} \quad (2)$$

where $\hat{\mathbf{I}}_k(\mathbf{r}) = \int d\mathbf{r}' \mathbf{F}(\mathbf{r} - \mathbf{r}') \hat{f}_k(\mathbf{r}) \hat{f}_0(\mathbf{r}')$. The ξ_k 's are centered Gaussian white noise fields, induced by the

individual noises $\zeta_i(t)$ entering Eq. (1b). They are given by $\xi_k(\mathbf{r}, t) = ik\sqrt{2D_r}\sum_i \zeta_i(t)e^{ik\theta_i}\delta[\mathbf{r} - \mathbf{r}_i(t)]$ and satisfy $\langle \xi_k(\mathbf{r}, t)\xi_q(\mathbf{r}', t') \rangle_{\zeta_i} = \hat{\Lambda}_{kq}\delta(t-t')\delta(\mathbf{r} - \mathbf{r}')$, with

$$\hat{\Lambda}_{kq} = -2kqD_r\hat{f}_{q+k}. \quad (3)$$

The bare mass of the orientation field \hat{f}_1 is thus equal to D_r . The fluctuations, however, induce a nonvanishing correction to this bare mass that we now compute.

To focus on the core mechanism, we consider the limit $v_0 = \mu = 0$ and $r_0 = \infty$ in Eq. (1), which amounts to studying N fully connected XY spins with nematic alignment. Equation (2) directly generalizes to this case, without the transport terms, with $\hat{f}_k(t)$ the k th Fourier mode of $\hat{\psi}(\theta) = \sum_i \delta(\theta - \theta_i)$, and with $\hat{f}_0 = N$. Therefore, the dynamics of the first two modes read

$$\dot{\hat{f}}_1 = -D_r\hat{f}_1 + \frac{\gamma}{2N}\hat{f}_2\hat{f}_{-1} - \frac{\gamma}{2N}\hat{f}_3\hat{f}_{-2} + \xi_1, \quad (4a)$$

$$\dot{\hat{f}}_2 = -(4D_r - \gamma)\hat{f}_2 - \frac{\gamma}{N}\hat{f}_4\hat{f}_{-2} + \xi_2. \quad (4b)$$

When $N \rightarrow \infty$, the mean-field approximation to the dynamics exactly predicts the relaxation of $f_k = \langle \hat{f}_k \rangle$. In the high-temperature phase, the stable fixed points correspond to $f_{k>0}^0 = 0$ and the masses of the polar and nematic fields are D_r and $4D_r - \gamma$, respectively. To compute the first-order correction to mean field, we evaluate $(\gamma/2N)\langle \hat{f}_2\hat{f}_{k-2} - \hat{f}_{-2}\hat{f}_{k+2} \rangle$ to leading order in N^{-1} . Rewriting the Fourier modes as $\hat{f}_k = f_k^0 + \delta f_k$ and using that $f_k^0 = 0$ in the high-temperature phase, one can expand the correlators to get

$$\partial_t f_k = -k^2 D_r f_k + \frac{k\gamma}{2N} (\langle \delta f_2 \delta f_{k-2} \rangle - \langle \delta f_{-2} \delta f_{k+2} \rangle). \quad (5)$$

Then, the linearized dynamics of the fluctuations in Fourier space read $\partial_t \delta f_k = -(k^2 D_r - \gamma \delta_{|k|,2}) \delta f_k + \xi_k$. Using Itô calculus, one then finds the steady-state correlators

$$\langle \delta f_k \delta f_q \rangle = \frac{\Lambda_{kq}}{(k^2 + q^2)D_r - \gamma(\delta_{|k|,2} + \delta_{|q|,2})}, \quad (6)$$

with $\Lambda_{kq} = \langle \hat{\Lambda}_{kq} \rangle$. This yields a renormalized dynamics for the modes given by $\partial_t f_k = -\mathbf{m}_k f_k + \mathcal{O}(f_k/N^2)$. For the polar and nematic fields, we get the renormalized masses

$$\mathbf{m}_1 = D_r - \frac{4\gamma D_r(\gamma - D_r)}{N(5D_r - \gamma)(13D_r - \gamma)} + \mathcal{O}\left(\frac{1}{N^2}\right), \quad (7a)$$

$$\mathbf{m}_2 = 4D_r - \gamma + \frac{16D_r\gamma}{N(20D_r - \gamma)} + \mathcal{O}\left(\frac{1}{N^2}\right). \quad (7b)$$

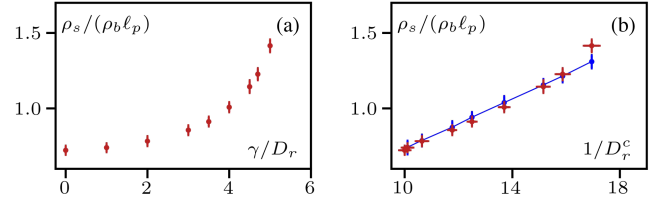


FIG. 2. (a) Ratio between boundary density and bulk density, ρ_s/ρ_b , normalized by the bare persistence ℓ_p as γ is varied and the bare rotational diffusivity D_r is kept constant. Measurements obtained from simulations of Eq. (1) without pairwise forces. (b) Red dots: same data as in panel (a), plotted against $1/D_r^c(\gamma)$, where $D_r^c(\gamma)$ is extracted from the fit of $C_M(t)$. Blue dots connected by a line: boundary accumulation of noninteracting particles whose bare rotational diffusivities D_r are chosen equal to the measured values of $D_r^c(\gamma)$ for the data of panel (a), as a function of $1/D_r = 1/D_r^c(\gamma)$.

As expected, fluctuations increase the mass of the nematic field, shifting the ordering transition to temperatures lower than the mean-field prediction $D_r = \gamma/4$. Surprisingly, however, Eq. (7) predicts that the mass of the polar field is *reduced* by fluctuations when $D_r < \gamma < 5D_r$ [67]. All in all, fluctuations thus suppress the nematic order while they favor the polar one.

While our results are perturbative, microscopic simulations reported in Supplemental Material, Fig. S2 [57] show these effects to hold nonperturbatively. Note that our results rely on the exact expression of the noise statistics, Eq. (3), which we derived in Eq. (2) from the microscopic dynamics, Eq. (1). As shown in [57], complementing a mean-field Landau theory by phenomenological uncorrelated noises would (wrongly) lead to the opposite prediction of an increase of \mathbf{m}_1 due to fluctuations.

The interplay between fluctuations and nematic torques thus leads to a reduction of the polar field mass. This general result, which also holds in equilibrium, implies that nematic torques enhance the persistence of active particles. Together with the phase diagrams shown in Fig. 1, this qualitatively explains how phase separation is either favored or suppressed by nematic torques. We now turn to check the validity of our predictions as well as their scope. Before considering the complex many-body dynamics of Eq. (1), we consider a simpler problem in which persistence plays a key role.

Boundary accumulation.—A typical trait of active particles is their tendency to accumulate at confining boundaries [2,18,68–71] where they spend a typical time of order τ before escaping to the bulk of the system. Dimensional analysis predicts that the ratio between surface and bulk densities—which scale as inverse surface and volume, respectively—should behave as $\rho_s/\rho_b \propto v_0\tau = \ell_p$, where ℓ_p is the persistence length. In Fig. 2(a), we show the results of simulations of Eq. (1) without interparticle forces, in the presence of a confining potential. As γ is increased up

to $\gamma \simeq 5D_r$, the fraction of particles at the walls increases by a factor of 2 while the system remains disordered. Our analytical computations suggest a simple qualitative explanation: aligning interactions lead to a reduced effective rotational diffusivity D_r^c . In turn, this yields an enhanced persistence length $\ell_p^c = v_0/D_r^c$ and thus an increased boundary accumulation.

To test this hypothesis, we measured the autocorrelation function of the total orientation, $\hat{\mathbf{M}}(t) \equiv \int d\mathbf{r} \hat{\mathbf{m}}(\mathbf{r}, t)$, in the presence of aligning torques: $C_M(t) \equiv \langle \hat{\mathbf{M}}(t) \cdot \hat{\mathbf{M}}(0) \rangle$. For $\gamma \leq 5D_r$, the system remains disordered and $C_M(t)$ is well fitted by an exponential decay $C_M(t) = \mathbf{M}_0^2 \exp(-D_r^c t)$, from which we extract $D_r^c(\gamma)$. As predicted, $D_r^c(\gamma)$ is a decreasing function of γ . We then compared the boundary accumulation with that observed in simulations of *non-interacting* particles with rotational diffusivity $D_r = D_r^c(\gamma)$. Remarkably, the excess densities are hardly distinguishable below $\gamma = 4.7D_r$, i.e., when the interacting system is far enough from the ordering transition [Fig. 2(b)]. The renormalization of the polar-field mass, which is a hydrodynamic effect, thus quantitatively accounts for the particle accumulation at the boundaries, despite the microscopic nature of this phenomenon.

Nematic torques and MIPS.—Let us now show that the renormalization of the polar-field mass also quantitatively accounts for the emergence of MIPS at finite γ . To do so, we first derive the relaxation dynamics of the density field. For $k=0$, Eq. (2) reads $\dot{\rho} = -\nabla \cdot \mathbf{J}$, where $\mathbf{J}(\mathbf{r}) = v_0 \mathbf{m}(\mathbf{r}) + \mu \mathbf{I}_0(\mathbf{r})$, $\mathbf{m} = \langle \hat{\mathbf{m}} \rangle$, and $\mathbf{I}_0(\mathbf{r}) = \langle \int d\mathbf{r}' \hat{\rho}(\mathbf{r}') \mathbf{F}(\mathbf{r} - \mathbf{r}') \hat{\rho}(\mathbf{r}') \rangle$. The dynamics of \mathbf{m} then stems from that of f_1 as

$$\begin{aligned} \partial_t \mathbf{m} = & -\nabla \cdot \left[v_0 \left(\mathbf{Q} + \frac{\rho \mathbb{I}}{2} \right) + \mu \mathbf{I}_1 \right] \\ & - D_r \mathbf{m} + \left\langle \frac{\gamma}{\hat{\rho}} \hat{\mathbf{Q}} \cdot \hat{\mathbf{m}} - \frac{2\gamma}{\hat{\rho}} \hat{\chi} \cdot \hat{\mathbf{Q}} \right\rangle, \end{aligned} \quad (8)$$

where $\mathbb{I}_{\alpha\beta} = \delta_{\alpha\beta}$, $\mathbf{I}_{1,\alpha\beta}(\mathbf{r}) = \langle \int d\mathbf{r}' \hat{m}_\beta(\mathbf{r}') F_\alpha(\mathbf{r} - \mathbf{r}') \hat{\rho}(\mathbf{r}') \rangle$, $\hat{\mathbf{Q}}_{\alpha\beta}(\mathbf{r}) = \sum_i [\mathbf{u}_{i,\alpha} \mathbf{u}_{i,\beta} - (\delta_{\alpha\beta}/2)] \delta(\mathbf{r} - \mathbf{r}_i)$ is the nematic order field, $\mathbf{Q} = \langle \hat{\mathbf{Q}} \rangle$, and $\hat{\chi}_{\alpha\beta\gamma}$ is a third-order tensor [57]. In general, closing Eq. (8) for the field \mathbf{m} is a difficult task. In light of our results, we predict that, in the high-temperature disordered phase, the nonlinear aligning terms can simply be accounted for by a renormalization of the bare mass D_r of the polar field. The nonconserving terms in Eq. (8) thus reduce to $-\mathbf{m}(\rho, \gamma) \mathbf{m}$. A fast variable treatment on \mathbf{m} then allows us to rewrite the dynamics of ρ as

$$\dot{\rho} = -\nabla \cdot \left[\mu \frac{D_r}{\mathbf{m}_1} \nabla \cdot \boldsymbol{\sigma}^a + \mu \nabla \cdot \boldsymbol{\sigma}^{\text{IK}} \right], \quad (9)$$

where we have introduced $\boldsymbol{\sigma}^a = -v_0^2 [\mathbf{Q} + (\rho \mathbb{I}/2)] / (\mu D_r) - v_0 \mathbf{I}_1 / D_r$ and followed Irving and Kirkwood to rewrite the contribution of pairwise forces as $\mathbf{I}_0 = \nabla \cdot \boldsymbol{\sigma}^{\text{IK}}$ [72,73]. To

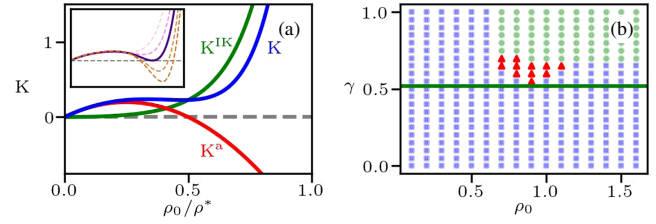


FIG. 3. Onset of MIPS. (a) Measurement of the active (red line) and passive (green line) components, K^a and K^{IK} , respectively, of the generalized bulk modulus K (blue line) as the density ρ_0 is varied, in the absence of nematic torques. The density is normalized by ρ^* , the density at which the effective self-propulsion speed $v(\rho) \equiv \langle \hat{\mathbf{r}}_i \cdot \mathbf{u}(\theta_i) \rangle$ vanishes. From the measurement of $\mathbf{m}_1(\rho_0, \gamma)$, Eq. (11) predicts the evolution of $K^{\text{th}}(\rho_0, \gamma)$ when γ is increased. Five representative curves are shown in the inset, with γ ranging from 0 to 0.6. The solid line corresponds to $\gamma_c = 0.52$. (b) Phase diagram corresponding to simulations of Eq. (1) as ρ_0 and γ are varied. Blue squares correspond to homogenous disorder systems. Red triangles correspond to the MIPS region. Green circles correspond to the emergence of nematic order. The solid green line corresponds to the theoretical prediction $\gamma_c = 0.52$.

assess the stability of an isotropic, homogeneous phase at density ρ_0 , we compute the linearized dynamics in Fourier space of a fluctuation along, say, the \hat{x} axis, which reads

$$\partial_t \delta \rho_q = \mu q^2 \left[\frac{D_r}{\mathbf{m}_1} \sigma_{xx}^a{}'(\rho_0) + \sigma_{xx}^{\text{IK}}{}'(\rho_0) \right] \delta \rho_q, \quad (10)$$

where the prime denotes derivative with respect to ρ_0 .

When $\gamma = 0$, $\boldsymbol{\sigma}^a$ is the contribution of the active forces to the stress tensor [70,74,75], $\mathbf{m}_1 = D_r$, and Eq. (9) reduces to $\dot{\rho} = -\nabla \cdot (\mu \nabla \cdot \boldsymbol{\sigma})$ [75]. The mechanical pressure exerted by active particles then satisfies an equation of state given by $P = -\text{Tr} \boldsymbol{\sigma} / 2$ and an isotropic homogeneous profile at density ρ_0 is linearly unstable whenever $P'(\rho_0) = -\sigma_{xx}^a{}'(\rho_0) - \sigma_{xx}^{\text{IK}}{}'(\rho_0) < 0$. This is the standard mechanical route to account for the MIPS induced by repulsive pairwise forces [28,32,75–77]. The system is thus unstable when its bulk modulus is negative: $K = \rho_0 P'(\rho_0) = K^a(\rho_0) + K^{\text{IK}}(\rho_0) < 0$, where K has been split into active and passive components $K^a(\rho_0) \equiv -\rho_0 \sigma_{xx}^a{}'(\rho_0)$ and $K^{\text{IK}}(\rho_0) \equiv -\rho_0 \sigma_{xx}^{\text{IK}}{}'(\rho_0)$.

In the presence of aligning torques, despite the lack of equation of state [78], K^a and K^{IK} still control the stability of homogeneous profiles through Eq. (10). This suggests defining a “generalized bulk modulus”—without connection to mechanics—as $K \equiv (D_r / \mathbf{m}_1) K^a + K^{\text{IK}}$. Like in equilibrium, negative values of K then lead to a spinodal decomposition. In the disordered phase, we expect that γ barely alters the values of K^a and K^{IK} (see Supplemental Material, Figs. S3a and S3b [57]). Their measurements at $\gamma = 0$, show that K^a favors instability whereas K^{IK} stabilizes homogeneous phases [see Fig. 3(a)]. Their sum is positive and the system is stable. As γ increases, we

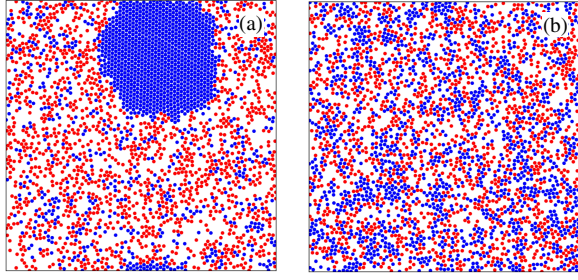


FIG. 4. Impact of nematic torques on mixtures of active particles (red circles) and passive particles (blue circles) evolving under Eqs. (12a) and (12b), respectively. (a) In the absence of nematic torques, passive particles undergo phase separation whenever the persistence length of the active particles is small enough. (b) Nematic alignment between the active particles ($\gamma = 4.5D_r$) suppresses the phase separation of the passive component.

estimate the generalized bulk modulus as

$$K^{\text{th}}(\rho_0, \gamma) \equiv K^{\text{IK}}(\rho_0) + \frac{D_r}{\mathbf{m}_1(\rho_0, \gamma)} K^{\text{a}}(\rho_0). \quad (11)$$

The renormalization of \mathbf{m}_1 thus enhances the contribution of K^{a} by a factor of (D_r/\mathbf{m}_1) . The inset of Fig. 3(a) shows $K^{\text{th}}(\rho_0, \gamma)$ for several values of γ . For $\gamma > \gamma_c = 0.52$, the active bulk modulus dominates and we predict the occurrence of MIPS. This is successfully compared with simulations of Eq. (1) in the (γ, ρ_0) plane in Fig. 3(b). All in all, the renormalization of \mathbf{m}_1 due to the nematic torques thus induces MIPS by increasing the active contribution to the bulk modulus.

Mixture of active and passive particles.—To show that our results apply more broadly, we consider mixtures of active and passive particles interacting via purely repulsive forces, which have attracted a lot of attention recently [79–85]. Active particles are characterized by positions \mathbf{r}_i^{a} and orientations $\mathbf{u}(\theta_i)$ while the positions of passive particles are denoted by \mathbf{r}_i^{p} . The spatial dynamics read

$$\dot{\mathbf{r}}_i^{\text{a}} = v_0 \mathbf{u}_i - \mu \sum_{|\mathbf{r}_i^{\text{a}} - \mathbf{r}_j^{\text{a}}| < r_0} \nabla U(\mathbf{r}_i^{\text{a}} - \mathbf{r}_j^{\text{a}}) - \mu \sum_{|\mathbf{r}_i^{\text{a}} - \mathbf{r}_j^{\text{p}}| < r_0} \nabla U(\mathbf{r}_i^{\text{a}} - \mathbf{r}_j^{\text{p}}), \quad (12a)$$

$$\dot{\mathbf{r}}_i^{\text{p}} = -\mu \sum_{|\mathbf{r}_i^{\text{p}} - \mathbf{r}_j^{\text{p}}| < r_0} \nabla U(\mathbf{r}_i^{\text{p}} - \mathbf{r}_j^{\text{p}}) - \mu \sum_{|\mathbf{r}_i^{\text{p}} - \mathbf{r}_j^{\text{a}}| < r_0} \nabla U(\mathbf{r}_i^{\text{p}} - \mathbf{r}_j^{\text{a}}), \quad (12b)$$

and the orientations of the active particles evolve according to Eq. (1b). In such mixtures, the passive component undergoes phase separation when the persistence length of the active particles is small enough [82], as shown in the simulation reported in Fig. 4(a) for $\gamma = 0$. Our results suggest that increasing γ should enhance the persistence of

the active particles, thereby vaporizing the dense passive phase. This is indeed what is reported in Fig. 4(b) where γ has been increased up to $\gamma/D_r \simeq 4.5$. This shows that the impact of nematic torques in disordered scalar matter can be generically accounted for by an increase of the persistence length.

Conclusion.—We have shown how fluctuations enhance polar order in collections of nematically aligning particles. In active systems, this leads to an increase of the persistence length, hence impacting emergent properties. As suggested by our hydrodynamic treatment, we expect this effect to be generic and to extend beyond systems described by Eq. (1). Supplemental Material Sec. V for instance show how nematic torques also enhance persistence in discrete-time Vicsek-like models [57]. Similar results should also apply to passive systems where, to the best of our knowledge, it has not been reported before. In experiments, increasing the density of active particles should generically lead to an increase of their persistence due to nematically aligning collisions, which should oppose the well-documented decrease of self-propulsion due to head-on collisions [23]. Note that our work uses the same range for pairwise forces and aligning torques, hence being as close as possible to collision-based models, where repulsive forces and aligning dynamics go hand in hand. For swarming bacteria like *B. subtilis*, we suspect that a difference in shapes between bacteria at the forefront and in the core of the colony could regulate the bacterial persistence and play an important role in the spreading of the swarm.

We thank Josep-Maria Armengol-Collado, François Graner, Yariv Kafri, Sunghan Ro, Alex Solon, and Fred van Wijland for stimulating discussions. J. T., C. D., and G. S. acknowledge support from the ANR grant THEMA. C. D. acknowledges the support of a postdoctoral fellowship and G. S. acknowledges the support of a doctoral fellowships from from the LabEx “Who Am I?” (ANR-11-LABX-0071) and the Université Paris Cité IdEx (ANR-18-IDEX-0001) funded by the French Government through its “Investments for the Future” program.

-
- [1] M. C. Marchetti, J.-F. Joanny, S. Ramaswamy, T. B. Liverpool, J. Prost, M. Rao, and R. A. Simha, *Rev. Mod. Phys.* **85**, 1143 (2013).
 - [2] C. Bechinger, R. Di Leonardo, H. Löwen, C. Reichhardt, G. Volpe, and G. Volpe, *Rev. Mod. Phys.* **88**, 045006 (2016).
 - [3] H. Chaté, *Annu. Rev. Condens. Matter Phys.* **11**, 189 (2020).
 - [4] J. O’Byrne, Y. Kafri, J. Tailleur, and F. van Wijland, *Nat. Rev. Phys.* **4**, 167 (2022).
 - [5] M. Ballerini, N. Cabibbo, R. Candelier, A. Cavagna, E. Cisbani, I. Giardina, V. Lecomte, A. Orlandi, G. Parisi, A. Procaccini, M. Viale, and V. Zdravkovic, *Proc. Natl. Acad. Sci. U.S.A.* **105**, 1232 (2008).

- [6] V. Schaller, C. Weber, C. Semmrich, E. Frey, and A. R. Bausch, *Nature (London)* **467**, 73 (2010).
- [7] C. Battle, C. P. Broedersz, N. Fakhri, V. F. Geyer, J. Howard, C. F. Schmidt, and F. C. MacKintosh, *Science* **352**, 604 (2016).
- [8] M. Poujade, E. Grasland-Mongrain, A. Hertzog, J. Jouanneau, P. Chavrier, B. Ladoux, A. Buguin, and P. Silberzan, *Proc. Natl. Acad. Sci. U.S.A.* **104**, 15988 (2007).
- [9] J. R. Howse, R. A. L. Jones, A. J. Ryan, T. Gough, R. Vafabakhsh, and R. Golestanian, *Phys. Rev. Lett.* **99**, 048102 (2007).
- [10] A. Bricard, J.-B. Caussin, N. Desreumaux, O. Dauchot, and D. Bartolo, *Nature (London)* **503**, 95 (2013).
- [11] D. Nishiguchi and M. Sano, *Phys. Rev. E* **92**, 052309 (2015).
- [12] J. Yan, M. Han, J. Zhang, C. Xu, E. Luijten, and S. Granick, *Nat. Mater.* **15**, 1095 (2016).
- [13] T. Vicsek, A. Czirók, E. Ben-Jacob, I. Cohen, and O. Shochet, *Phys. Rev. Lett.* **75**, 1226 (1995).
- [14] J. Toner and Y. Tu, *Phys. Rev. Lett.* **75**, 4326 (1995).
- [15] S. Ngo, A. Peshkov, I. S. Aranson, E. Bertin, F. Ginelli, and H. Chaté, *Phys. Rev. Lett.* **113**, 038302 (2014).
- [16] A. P. Solon, H. Chaté, and J. Tailleur, *Phys. Rev. Lett.* **114**, 068101 (2015).
- [17] P. Galajda, J. Keymer, P. Chaikin, and R. Austin, *J. Bacteriol.* **189**, 8704 (2007).
- [18] J. Tailleur and M. Cates, *Europhys. Lett.* **86**, 60002 (2009).
- [19] R. Di Leonardo, L. Angelani, D. Dell'Arciprete, G. Ruocco, V. Iebba, S. Schippa, M. P. Conte, F. Mecarini, F. De Angelis, and E. Di Fabrizio, *Proc. Natl. Acad. Sci. U.S.A.* **107**, 9541 (2010).
- [20] A. Sokolov, M. M. Apodaca, B. A. Grzybowski, and I. S. Aranson, *Proc. Natl. Acad. Sci. U.S.A.* **107**, 969 (2010).
- [21] S. C. Takatori, R. De Dier, J. Vermant, and J. F. Brady, *Nat. Commun.* **7**, 10694 (2016).
- [22] Y. Baek, A. P. Solon, X. Xu, N. Nikola, and Y. Kafri, *Phys. Rev. Lett.* **120**, 058002 (2018).
- [23] Y. Fily and M. C. Marchetti, *Phys. Rev. Lett.* **108**, 235702 (2012).
- [24] G. S. Redner, M. F. Hagan, and A. Baskaran, *Phys. Rev. Lett.* **110**, 055701 (2013).
- [25] J. Stenhammar, D. Marenduzzo, R. J. Allen, and M. E. Cates, *Soft Matter* **10**, 1489 (2014).
- [26] A. Wysocki, R. G. Winkler, and G. Gompper, *Europhys. Lett.* **105**, 48004 (2014).
- [27] M. E. Cates and J. Tailleur, *Annu. Rev. Condens. Matter Phys.* **6**, 219 (2015).
- [28] A. P. Solon, J. Stenhammar, M. E. Cates, Y. Kafri, and J. Tailleur, *Phys. Rev. E* **97**, 020602(R) (2018).
- [29] P. Digregorio, D. Levis, A. Suma, L. F. Cugliandolo, G. Gonnella, and I. Pagonabarraga, *Phys. Rev. Lett.* **121**, 098003 (2018).
- [30] C. B. Caporusso, P. Digregorio, D. Levis, L. F. Cugliandolo, and G. Gonnella, *Phys. Rev. Lett.* **125**, 178004 (2020).
- [31] A. K. Omar, K. Klymko, T. GrandPre, and P. L. Geissler, *Phys. Rev. Lett.* **126**, 188002 (2021).
- [32] T. Speck, *Phys. Rev. E* **103**, 012607 (2021).
- [33] D. Saintillan and M. J. Shelley, *Phys. Rev. Lett.* **100**, 178103 (2008).
- [34] J. Tailleur and M. E. Cates, *Phys. Rev. Lett.* **100**, 218103 (2008).
- [35] S. Saha, R. Golestanian, and S. Ramaswamy, *Phys. Rev. E* **89**, 062316 (2014).
- [36] R. Zakine, J.-B. Fournier, and F. Van Wijland, *Phys. Rev. Lett.* **121**, 028001 (2018).
- [37] J. Deseigne, O. Dauchot, and H. Chaté, *Phys. Rev. Lett.* **105**, 098001 (2010).
- [38] V. Schaller, C. A. Weber, B. Hammerich, E. Frey, and A. R. Bausch, *Proc. Natl. Acad. Sci. U.S.A.* **108**, 19183 (2011).
- [39] F. Peruani, J. Starruß, V. Jakovljevic, L. Søgaaard-Andersen, A. Deutsch, and M. Bär, *Phys. Rev. Lett.* **108**, 098102 (2012).
- [40] Y. Sumino, K. H. Nagai, Y. Shitaka, D. Tanaka, K. Yoshikawa, H. Chaté, and K. Oiwa, *Nature (London)* **483**, 448 (2012).
- [41] D. Geyer, D. Martin, J. Tailleur, and D. Bartolo, *Phys. Rev. X* **9**, 031043 (2019).
- [42] F. Peruani, T. Klauss, A. Deutsch, and A. Voss-Boehme, *Phys. Rev. Lett.* **106**, 128101 (2011).
- [43] F. D. C. Farrell, M. C. Marchetti, D. Marenduzzo, and J. Tailleur, *Phys. Rev. Lett.* **108**, 248101 (2012).
- [44] C. A. Weber, T. Hanke, J. Deseigne, S. Léonard, O. Dauchot, E. Frey, and H. Chaté, *Phys. Rev. Lett.* **110**, 208001 (2013).
- [45] E. Sese-Sansa, I. Pagonabarraga, and D. Levis, *Europhys. Lett.* **124**, 30004 (2018).
- [46] X. Shi and H. Chaté, [arXiv:1807.00294](https://arxiv.org/abs/1807.00294).
- [47] R. Van Damme, J. Rodenburg, R. Van Roij, and M. Dijkstra, *J. Chem. Phys.* **150**, 164501 (2019).
- [48] M. N. Van Der Linden, L. C. Alexander, D. G. A. L. Aarts, and O. Dauchot, *Phys. Rev. Lett.* **123**, 098001 (2019).
- [49] R. Großmann, I. S. Aranson, and F. Peruani, *Nat. Commun.* **11**, 5365 (2020).
- [50] E. Sesé-Sansa, D. Levis, and I. Pagonabarraga, *Phys. Rev. E* **104**, 054611 (2021).
- [51] R. A. Simha and S. Ramaswamy, *Phys. Rev. Lett.* **89**, 058101 (2002).
- [52] J. Toner, Y. Tu, and S. Ramaswamy, *Ann. Phys. (Amsterdam)* **318**, 170 (2005).
- [53] F. Ginelli, F. Peruani, M. Bär, and H. Chaté, *Phys. Rev. Lett.* **104**, 184502 (2010).
- [54] D. Nishiguchi, K. H. Nagai, H. Chaté, and M. Sano, *Phys. Rev. E* **95**, 020601(R) (2017).
- [55] S. Shankar, S. Ramaswamy, and M. C. Marchetti, *Phys. Rev. E* **97**, 012707 (2018).
- [56] B. Mahault and H. Chaté, *Phys. Rev. Lett.* **127**, 048003 (2021).
- [57] See Supplemental Material at <http://link.aps.org/supplemental/10.1103/PhysRevLett.132.078301>, which includes theoretical and numerical details, as well as Refs. [58–64].
- [58] D. Martin, H. Chaté, C. Nardini, A. Solon, J. Tailleur, and F. Van Wijland, *Phys. Rev. Lett.* **126**, 148001 (2021).
- [59] D. S. Dean, *J. Phys. A* **29**, L613 (1996).
- [60] M. Doi, *J. Polym. Sci.* **19**, 229 (1981).

- [61] D. Martin, J. O'Byrne, M. E. Cates, É. Fodor, C. Nardini, J. Tailleur, and F. van Wijland, *Phys. Rev. E* **103**, 032607 (2021).
- [62] A. Patelli, I. Djafer-Cherif, I. S. Aranson, E. Bertin, and H. Chaté, *Phys. Rev. Lett.* **123**, 258001 (2019).
- [63] R. Kürsten and T. Ihle, *Phys. Rev. E* **104**, 034604 (2021).
- [64] Y.-L. Chou and T. Ihle, *Phys. Rev. E* **91**, 022103 (2015).
- [65] P. M. Chaikin and T. C. Lubensky, *Principles of Condensed Matter Physics* (Cambridge University Press, Cambridge, England, 1995), Vol. 10.
- [66] A. Peshkov, E. Bertin, F. Ginelli, and H. Chaté, *Eur. Phys. J. Spec. Top.* **223**, 1315 (2014).
- [67] Note that the computations leading to Eq. (7) are valid only in the disordered phase, where $\gamma \leq 4D_r$, so that the spurious divergences predicted in Eq. (7) are never observed.
- [68] J. Elgeti and G. Gompper, *Europhys. Lett.* **85**, 38002 (2009).
- [69] Y. Fily, A. Baskaran, and M. F. Hagan, *Soft Matter* **10**, 5609 (2014).
- [70] X. Yang, M. L. Manning, and M. C. Marchetti, *Soft Matter* **10**, 6477 (2014).
- [71] A. Deblais, T. Barois, T. Guerin, P.-H. Delville, R. Vaudaine, J. S. Lintuvuori, J.-F. Boudet, J.-C. Baret, and H. Kellay, *Phys. Rev. Lett.* **120**, 188002 (2018).
- [72] J. Irving and J. G. Kirkwood, *J. Chem. Phys.* **18**, 817 (1950).
- [73] M. Krüger, A. Solon, V. Démery, C. M. Rohwer, and D. S. Dean, *J. Chem. Phys.* **148**, 084503 (2018).
- [74] S. C. Takatori, W. Yan, and J. F. Brady, *Phys. Rev. Lett.* **113**, 028103 (2014).
- [75] A. P. Solon, J. Stenhammar, R. Wittkowski, M. Kardar, Y. Kafri, M. E. Cates, and J. Tailleur, *Phys. Rev. Lett.* **114**, 198301 (2015).
- [76] A. P. Solon, J. Stenhammar, M. E. Cates, Y. Kafri, and J. Tailleur, *New J. Phys.* **20**, 075001 (2018).
- [77] A. K. Omar, H. Row, S. A. Mallory, and J. F. Brady, *Proc. Natl. Acad. Sci. U.S.A.* **120**, e2219900120 (2023).
- [78] A. P. Solon, Y. Fily, A. Baskaran, M. E. Cates, Y. Kafri, M. Kardar, and J. Tailleur, *Nat. Phys.* **11**, 673 (2015).
- [79] F. Alaimo and A. Voigt, *Phys. Rev. E* **98**, 032605 (2018).
- [80] J. Stenhammar, R. Wittkowski, D. Marenduzzo, and M. E. Cates, *Phys. Rev. Lett.* **114**, 018301 (2015).
- [81] S. C. Takatori and J. F. Brady, *Soft Matter* **11**, 7920 (2015).
- [82] S. N. Weber, C. A. Weber, and E. Frey, *Phys. Rev. Lett.* **116**, 058301 (2016).
- [83] A. Wysocki, R. G. Winkler, and G. Gompper, *New J. Phys.* **18**, 123030 (2016).
- [84] R. Wittkowski, J. Stenhammar, and M. E. Cates, *New J. Phys.* **19**, 105003 (2017).
- [85] P. Dolai, A. Simha, and S. Mishra, *Soft Matter* **14**, 6137 (2018).